LIGHT ION SOURCES FOR ICF*

R. A. Gerber, K. W. Bieg, E. J. T. Burns,
P. L. Dreike, J. Maenchen, T. A. Mehlhorn,
J. N. Olsen, A. L. Pregenzer, J. K. Rice,
M. A. Sweeney, G. C. Tisone, and J. R. Woodworth

Sandia National Laboratories
Albuquerque, NM 87185

Abstract

PBFA II, Sandia National Laboratories' (SNLA) advanced light-ion accelerator [1] (now under construction), will deliver a 30-MV, 5 MA lithium ion beam to an Inertial Confinement Fusion (ICF) target. Although most ICF experiments have been performed with proton beams, lithium ions were selected for PBFA II for several reasons. The use of lithium enables a large anode-cathode spacing, resulting in less impedance change during the pulse. Lithium ions have less magnetic deflection in the diode, so they can be focused for a longer period of time. Also, since the ionization potential of Li^+ is low, while that of L^{++} is very large, a Li^+ source should be achievable without significant contamination from Li^{++}. Ions heavier than Li^+ would require operating voltages greater than 30 MV, or the ions would have to be accelerated in a multiple charged state.

The selection of the lithium option for PBFA II has made the development of a suitable lithium source one of the highest priority areas in the light-ion ICF program. Following that decision in the fall of 1983, SNLA organized a comprehensive ion source program to develop an optimum lithium source for PBFA II and to understand near-term sources. The source requirements for the PBFA-II Applied-B diode are:

- $N^+ \approx 10^{16}$ cm^{-2}
- Plasma thickness ($\approx$ mm)
- $N^+/N > 50\%$
- Beam purity $> 90\%$ Li^+
- Operational in vacuum of 5×10^{-5} Torr
- Onset of ion current must be rapid

A source with these characteristics must be developed before target experiments begin in 1987. Our research on laser-produced sources, lithium guns, and liquid Li metal/salts will determine if these concepts can satisfy optimum source requirements. Research and development of near-term lithium flashover sources for the initial pulse power tests on PBFA II are also significant parts of the ion source program. These non-optimized sources will allow us to gain experience with Li-ion diodes and will enable development and optimization of non-protonic diagnostics. In addition to research on both near-term and optimum lithium sources, techniques are being developed to clean and preionize anode surfaces. These techniques include glow discharge, XUV flash, ambient heating, and pulse heating.

In addition to the SNLA ion source development approaches described here, research on non-protonic ion sources for ICF is being pursued at Cornell University and GT Devices. This paper will present

recent results on near-term lithium flashover sources, XUV illumination sources, and laser-produced lithium sources (BOLVAPS/LIBORS).

Lithium-Flashover Sources

The most popular and widely used source in ion diodes is the flashover source. This is a completely passive source in which the plasma is formed on a dielectric-filled anode during the operation of the diode. Although the plasma formation processes have been studied extensively, the exact mechanism is still not fully understood. We speculate that electron leakage to the anode contributes to surface breakdown by generating electric fields with large tangential components at a dielectric surface. The impact of both primary and secondary electrons on the dielectric surface desorbs neutrals. Neutral desorption by electron impact, which has a yield four to six orders of magnitude larger than ion desorption, [2] accounts for the efficiency of the plasma formation mechanism. The desorbed neutrals are subsequently ionized by avalanche electrons.

A common procedure used to fabricate a flashover source for hydrogen and carbon ions is to machine grooves in the anode and fill these grooves with a dielectric material such as epoxy or carnauba wax. Similar techniques have been used for lithium sources by using lithium-salt dielectrics. An Applied-B diode is being used on a Nereus accelerator [500-kV, 35-kA, 35-ns (FWHM) power pulse] to investigate lithium ion sources. RF glow discharge cleaning of the anode surface has also been implemented.

Lithium fluoride (LiF) was chosen as one of the dielectrics because it is less hygroscopic than most salts, it does not contain elements (e.g., nitrogen) with charge states that would interfere with the Li^+ analysis of a Thomson parabola particle analyzer, and many of the properties of LiF are known. Because LiF cannot be melted directly into the aluminum anode grooves because of its high melting temperature, we vacuum evaporate a thin coating of LiF over a conventional epoxy-filled, grooved anode. A coating thickness of 3 μm has been selected, as this is thicker than the range of secondary electrons and photons believed responsible for desorption.

Ion species obtained from both uncleaned LiF anodes and anodes cleaned with various glow-discharge treatments are shown in Table I. Relative ion species currents were determined by a Thomson parabola analysis of ion damage tracks produced on CR39 recording plastic. For an uncleaned LiF anode, approximately one quarter of the ion beam was extracted as Li^+. The F^+ current was about 64% of the observed lithium ion current. The ratio of these currents is consistent with Child-Langmuir, space-charge-limited emission from a plasma containing a stoichiometric composition of Li^+ and F^+. The lithium purity of the beam was increased substantially, to more than 50%, and the proton current decreased by glow discharge cleaning. The most effective gas for this purpose was 80% argon and 20% oxygen. As

expected, the carbon ion current was reduced correspondingly, presumably by the formation of volatiles (CO, CO_2). With delayed (1-3 min) pulsings, the lithium current remained high, suggesting that anode recontamination after glow discharge cleaning may not be a serious problem.

TABLE I

Anode treatment	H^+	Li^+	$C^{+,++}$	$O^{+,++}$	F^{++}	Other
Uncleaned	25	28	20	2	18	7
Ar glow, active	30	25	3	2	9	31
O_2 - 20% CF_4 glow	28	45	12	4	2	9
Ar - 20% O_2 glow	20	52	3	3	9	13
Ar - 20% O_2 glow, 1-3 min delay	11	60	8	9	7	5

Ion species from 3 μm LiF-coated, epoxy-filled grooved anode

The rf-cleaned, LiF-coated anode is a higher impedance source than the conventional epoxy-filled, flashover anode, resulting in substantially reduced diode and total ion currents. This high impedance operation may be caused by either reduced secondary electron and neutral desorption yields from a clean LiF surface or glow discharge modification of the LiF surface so as to inhibit anode plasma formation.

These experiments using the Nereus accelerator have demonstrated that a beam with greater than 50% Li^+ can be generated in an Applied-B diode. If the ion current density can be increased, this source would satisfy our near-term PBFA-II requirements.

Several ion diode experiments in which the anode grooves were filled with solid lithium nitrate ($LiNO_3$) were previously performed with limited success. Ion currents from these experiments showed a lithium ion content of 20% to 30% but with many contaminants such as hydrogen, carbon, and oxygen. [3] Recently an experiment was done using a liquid-lithium nitrate-filled anode. Liquids can deform under the competing effects of surface tension and electrostatic stress when subjected to a high electric field. This deformation can greatly enhance the electric field over portions of the surface, causing field desorption of ions. This is the same principle that underlies the operation of liquid metal capillary sources, which have produced a single, bright ion beam. [4] Notably, such a source does not depend on leakage electrons from the cathode. Moreover, liquid lithium nitrate should contain less water vapor and result in a beam with fewer surface impurities.

The major difference between this experiment on the PROTO-I accelerator (1.7 MV, 400 kA) and that described in Ref. 3 is that the lithium nitrate was suspended in vertical, fritted pyrex strips rather than in conventional grooves. The 10-cm-radius anode had 120 pyrex strips, each 4.0 mm wide, separated by 1.8 mm of aluminum. A photograph of the anode is shown in Fig. 1. A reservoir filled with solid lithium nitrate was located in the lower section of the anode. After the diode was evacuated, the anode was heated above the melt point of lithium nitrate (260 C), at which time the liquid began to wick up the fritted material. For the liquid-filled anode shots, the temperature was increased to 320 C and maintained until the liquid had completely filled the fritted material. For the solid lithium nitrate shots, the same procedure was used, except that the anode was allowed to cool in the diode until it reached about 200 C.
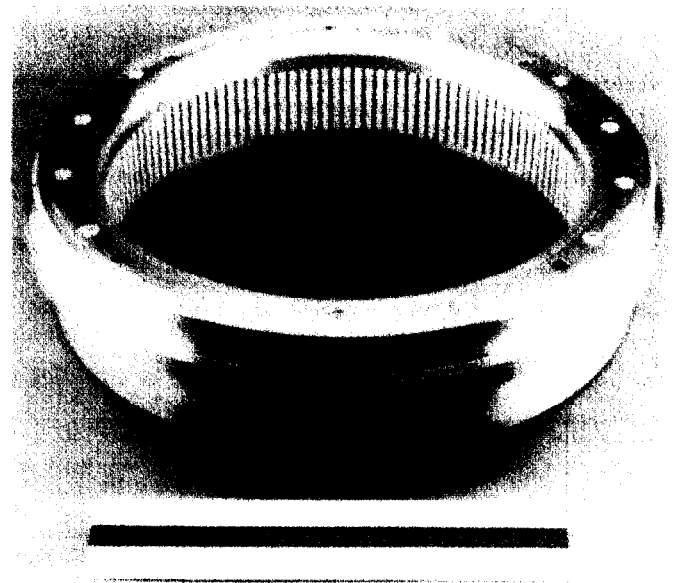
Figure 1: Photograph of PROTO I anode used for the lithium experiments. A reservoir containing solid lithium nitrate is located in the lower section.

Because our main interest was in species identification, a Thomson parabola analyzer was the major diagnostic. This instrument was equipped with CR-39 nuclear-track-recording plastic so that ion species abundances could be compared quantitatively by counting individual particle tracks. A gold foil scatterer intercepted part of the beam and scattered a small fraction of the ions into the collimator of the analyzer. A computer model has been developed to simulate scattering, charge exchange, and energy loss processes in the Rutherford scattering/Thomson parabola system. This code allows correlation of the observed parabola traces with the complete time-history of the voltage-current pulse.

Table II shows peak total current and ion current for the lithium shots. The majority of the shots were done with an anode-cathode spacing of 8.5 mm. Because of the low ion currents at this spacing, the cathode plates were extended to close the gap to 6.6 mm. The peak voltage was 1.9 MV for the 8.5 mm spacing and 1.7 MV for the 6.6 mm spacing.

TABLE II

Shot No.	Anode Dielectric	AK Gap (mm)	I_{Tot} (kA)	I_{ion} (kA)
4722	Liquid	8.5	245	30
4727	Liquid	8.5	285	35
4728	Solid	8.5	315	63
4729	Solid	8.5	295	40
4740	Liquid	6.6	380	135
4741	Solid	6.6	400	245
4743	Liquid	6.6	385	170

Summary of the PROTO I lithium ion diode experiments

Ion species analyses were done on three of the lithium nitrate shots, two liquid (4727 and 4743) and one solid (4728). The analysis was difficult and subject to error because of the low ion current density. Analysis of shot 4727 (AK gap = 8.5 mm) gave 80% to 90% Li^+ and 10% to 20% O^{3+}, with a probable current level of 10 to 25 kA. When the anode-cathode gap was decreased to 6.6 mm (shot 4743), the ion current was 170 kA. The ion analysis for this shot showed no Li^+, 10% H^+, 50% carbon, and 30% oxygen. The anode plasma turn-on mechanism may be

fundamentally different for different A-K gap spacings. The low-current shot had characteristics that could indicate plasma formation by field desorption of ions, while the higher-current case may be the normal anode turn-on mechanism of leakage electron currents.

An ion analysis of a solid lithium nitrate-filled anode shot (4728) indicates 30% to 40% Li^+ and 40% to 50% 0^{3+}, with the rest Si, N, and SiO_2 ions. Hydrogen and carbon, normally found with flashover sources, were absent in both low current shots (4727 and 4728). Further studies of liquid lithium nitrate and liquid Li metal, which are both candidates for field desorption of ions, are needed to establish the turn-on mechanisms and the feasibility of liquid Li^+ sources for PBFA II.

XUV Photon Sources

Surface discharges have been previously studied as UV photon sources for pumping lasers [5] for X-ray laser research [6] and as plasma sources for particle beam fusion experiments. [7]

In our experiments we want to determine whether XUV sources can be scaled to the required intensities to preionize or clean the anodes in particle beam diodes ($\sim$ 50 kW/cm^2 on the anode surface), while maintaining multiple shot capability and with a reasonably small power source.

The surface discharge electrodes, which are normally operated in vacuum ($< 5 \times 10^{-5}$ Torr), are built into the end of a stripline. The XUV sources are driven by discharging a capacitor bank through the stripline, producing a ringing current waveform. XUV light is obtained only during the first half cycle of the current waveform.

The 5.5-mm-long surface discharges themselves are formed between two copper electrodes attached to a glass fiber/polyimide-base insulator with epoxy. UV light emitted by the surface discharges are detected by four photodiodes. The "near UV" diode is a vacuum photodiode whose sensitivity extended from 8 eV to 4 eV. An array of three windowless photodiodes detects photons at energies above 10 eV. One diode has no filter, one diode is behind a 0.8-mm-thick aluminum filter, and the third is behind a 0.33-mm-thick parylene filter. These windowless diodes allowed us to determine the XUV photon energy in each of three spectral regions: 10 to 20 eV, 20 to 70 eV, and above 70 eV.

Table III shows the input parameters and light output of identical single-gap surface discharges driven by three different capacitor banks. Peak output power and total energy are shown as output into all space. The discharges are almost isotropic radiators with power and energy slightly peaked in the forward direction according to a $(\cos^{1/3} \theta)$ power-law. Table III also lists the efficiency of each discharge (efficiency = photon energy out/energy stored in capacitor bank). For each driving circuit the peak power and total energy per pulse varied as the square of the voltage on the capacitor bank (and hence with the square of the current through the discharge). Note that one surface discharge radiated a peak XUV power of over 80 MW and a total XUV energy of 60 Joules per pulse. The sources could be pulsed 15 to 20 times at this level before electrode erosion terminated their useful lifetime.

TABLE III						
DRIVING CIRCUIT				LIGHT OUTPUT		
C (μF)	V (kV)	$I_{(max)}$ (kA)	Energy (Joules)	$P_{(max)}$ (MW)	Energy (Joules)	Efficiency (%)
0.25	25	41	78	4	1.2	1.5
1.8	25	112	560	27	18	3.2
2.9	45	250	2900	81	60	2.1

XUV output versus driving circuit

Table IV shows the spectral results from an experiment using the 2.9-μF capacitor bank. These results are consistent with the discharge being an expanding, cooling plasma. Because the plasma is cooling, peak intensities for different wavelengths occur at different times. The discharge has an equivalent blackbody temperature between 5 and 6 eV at the time of peak output power.

TABLE IV					
Spectral Range (eV)	Above 70	70-20	20-10	8-4	Total
Peak Intensity (MW)	3.9	46	33	3	81
Total Energy (J)	0.6	18	37	4.5	60
FWHM of Light (ns)	150	380	680	1200	

XUV output with 2.9-μF capacitor bank

Based on the successful scaling results, we have designed an XUV discharge source for the Applied-B diode on PBFA I. In this design, 16 discharges, driven by eight capacitor banks, illuminate the entire anode with a peak XUV intensity of ~30 kW/cm^2. A schematic of the apparatus is shown in Fig. 2. On two different Applied-B diode shots, this configuration gave a nearly constant diode impedance of 1.0 to 0.7 Ω during most of the accelerator power pulse and the highest ion beam energy ever coupled through an Applied-B diode. Figure 3 compares power flow for shots with and without XUV illumination.
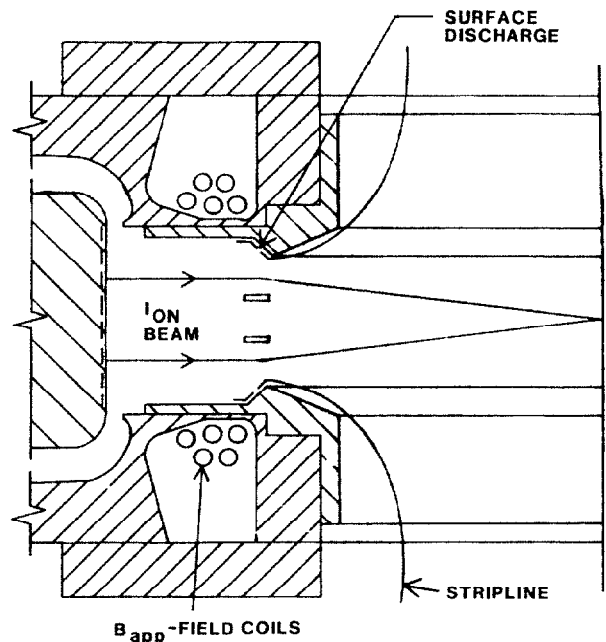
Figure 2. Schematic of XUV discharge source configurations in Applied-B diode for PBFA I proof-of-principle experiments.

PBFA POWER COMPARISON
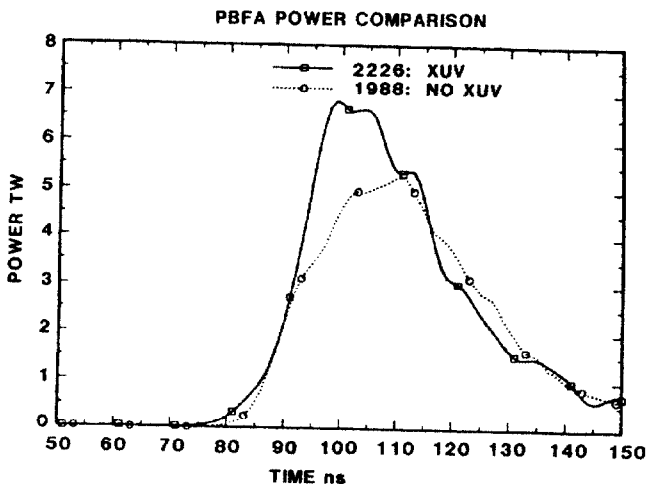
Figure 3. Comparison of PBFA-I diode power with and without XUV.

Recent calculations [8] suggest the XUV flux levels used on PBFA I (30-50 kW/cm^2) are high enough to melt a surface layer on the carnauba wax filled anodes used in PBFA I, but too low to melt the surface of anodes containing lithium. Therefore, we are investigating ways to increase the XUV flux level. Experiments at other laboratories [9] suggest surface discharges over cryogenic insulators, such as solid xenon, may produce XUV photons with an efficiency ~10-20 times higher than in our experiments. We have constructed an apparatus to examine the XUV output of cryogenic-insulator discharges.

Laser Produced Lithium Sources

A leading candidate for the optimum ion source for PBFA-II target experiments is the BOLVAPS/LIBORS scheme. BOLVAPS is a way to produce a thin lithium vapor layer near the anode surface by rapid ohmic heating of a thin-film laminate containing lithium. The vapor would then be ionized by LIBORS, [10] a laser technique producing a singly ionized lithium plasma. A sketch of the two phases of the BOLVAPS/LIBORS scheme is shown in Fig. 4. Recent experiments have demonstrated each process independently. A schematic diagram of the small-scale BOLVAPS experiment is shown in Fig. 5. Lithium is evaporated from a layer of 40 atomic-percent lithium in silver, which is about 1-μm thick and sputtered onto a 5-cm long, 2-cm wide, and 0.0025-cm thick tantalum foil. The foil, preheated by the "slow" capacitor bank (2.5-ms pulse duration) to a temperature of about 800 C, melts the LiAg and desorbs water. After a delay of a few ms, the foil is heated to a temperature of over 1000 C by a "fast" capacitor bank (8-μs half-cycle time). The lithium vapor density is measured using a two-photon-pumped fluorescence technique, indicated in Fig. 5. Measurements of the lithium density versus time into the fast pulse at a distance of 2 mm in front of the foil is shown in Fig. 6. A lithium vapor layer with a density in the 10^{15} - 10^{16} cm^{-3} range that is a few mm thick is evolved in a period of about 5 μs. The vapor layer thickness is consistent with the heating time and the ~1 mm/μs thermal velocity.

We believe the appropriate interpretation of these results is that an initial experiment has shown BOLVAPS can provide a lithium layer thin enough and

dense enough to serve as an anode plasma. The experiment has not explored the limits of the technique. For example, the samples can be heated to temperatures of > 1400 C in 3 μs, before heating is terminated by an arc. Light from the arc interferes with the fluorescence diagnostic, but one would expect to have a vapor layer about 1-mm thick, with a peak density > 10^{17} cm^{-3}.
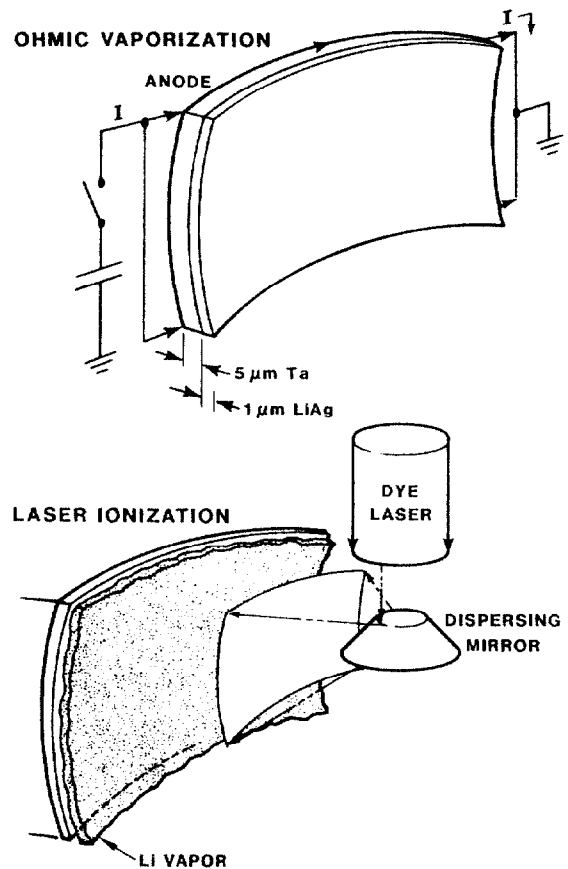
Figure 4: Sketch of two elements of BOLVAPS/LIBORS source.
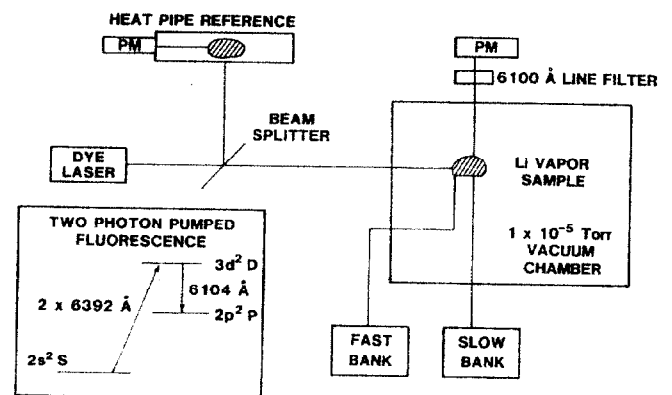
Figure 5: Diagram of the BOLVAPS demonstration experiment.

Li DENSITY vs. TIME
(d = 2 mm)
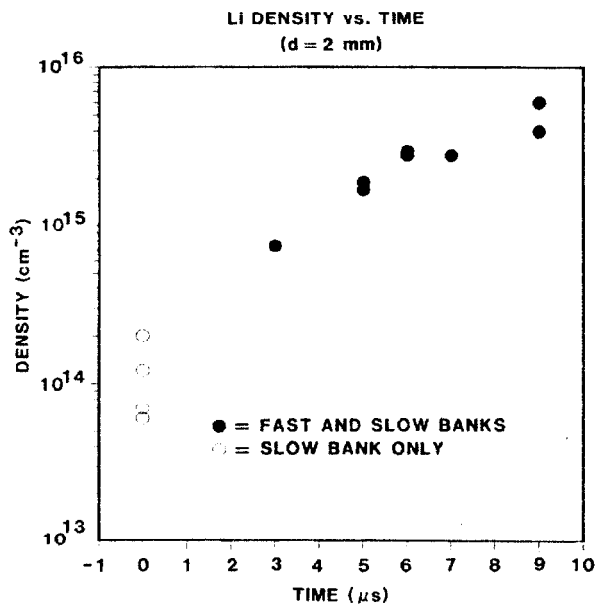
Figure 6: Measurements of lithium density in time from BOLVAPS.

Starting from the BOLVAPS-established vapor, Laser Ionization Based on Resonant Saturation (LIBORS) offers the possibility of a high density, pure, singly ionized ion source. Early work on laser-produced plasmas employed nonresonant excitation that required high-power pulsed lasers. In 1970 Measures [10] suggested plasmas could be produced more efficiently if the resonant transition in the vapor were excited by the laser. McIlrath and Lucatorto [11] achieved nearly 95% ionization in Li vapor with a 1-MW pulsed dye laser tuned to 670.8 nm. The ionization process starts when the resonant transition has been saturated by the laser. A few free electrons are formed by multi-photon ionization from the resonance level, laser-induced Penning ionization, or associative ionization. These electrons, heated via superelastic de-excitation collisions of the resonance level, can quickly ionize the excited atoms by direct collisional ionization of the resonance level and by populating intermediate levels that can then be ionized by single photons. As the electron density increases, electron collisions tend to bring the intermediate levels into LTE with the resonance level population. The result is very rapid and nearly complete ionization of the gas.

A detailed LIBORS model for lithium has been developed. This five-level, three-temperature model for laser ionization of Li vapor includes a one-dimensional description of the laser radiation transport and motion of the ionization front, coupled with a rate-equation description of the ionization and recombination processes. The model can handle realistic laser line shapes and has been used to predict laser requirements for PBFA-II type diodes.

We have an experimental program to study the ionization processes under conditions suitable for an ion source. A Li heat pipe provides a well-characterized Li vapor at a known temperature and density. Experiments have measured the time dependence of the transmission of the incident laser pulse through the vapor. The output of a flashlamp-pumped dye laser, tuned to the resonant line at 670.8 nm, is passed through the vapor. The time to ionize the vapor column (the burnthrough time) is then measured as a function of laser intensity and vapor density. These measurements are shown in Fig. 7 and

are compared with the model calculations. The agreement is excellent, giving us confidence that we can accurately predict laser requirements for a PBFA-II source. A detailed physics and engineering study was done to determine the feasibility of fielding a BOLVAPS/LIBORS source on PBFA II. The main limit on source performance is the attainable ohmic heating rate, which is limited by gas breakdown through the lithium vapor. The study indicates that a BOLVAPS/LIBORS lithium source could be fielded on PBFA II.

Summary

Lithium source requirements have been outlined for the advanced ICF accelerator, PBFA II. Sources have been identified for both near-term and target experiments, and recent experimental results were presented.
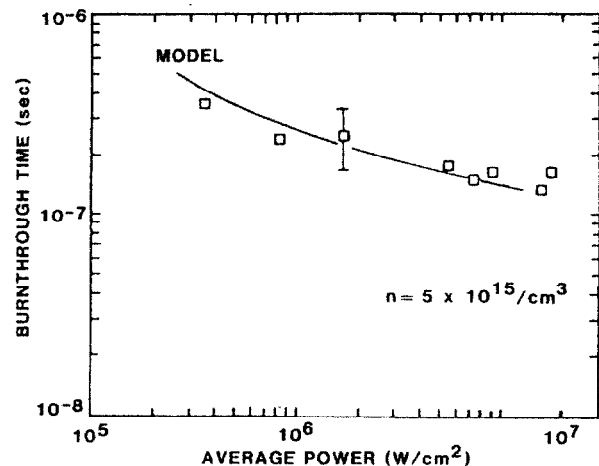
Figure 7: Comparison of the model calculations and experimentally measured burnthrough times as a function of dye laser intensity.

References

[1] D. L. Johnson, E. L. Neau, Proc. Fourth Int'l Pulsed Power Conf., Albuq, NM, (1983).

[2] J. Halbritter, J. Appl. Phys. 53 6475 (1982), IEEE Trans. on Electrical Insulation EI-18 253 (1983) and R. A. Anderson, Appl. Phys. Lett. 24, 54 (1974).

[3] G. S. Mills, E. J. T. Burns, and D. J. Johnson, Proc. 1984 IEEE Int'l Conf. on Plasma Science (1984).

[4] R. J. Pfeifer and C. D. Hendricks, Jr., AIAA Journal 6, 496, (1968).

[5] R. E. Beverly III, Progress in Optics 16, (350), North-Holland Publishing Co., New York, 1978.

[6] S. S. Glaros, S. L. Wong and G. L. James, Bull. Am. Phys. Soc. 27, 981 (1982).

[7] G. S. Mills, Bull. Am. Phys. Soc. 26, 988 (1981).

[8] M. A. Sweeney, Sandia National Laboratories (private communication).

[9] Y. T. Lie, P. Bogeni, and E. Hintz, Proc. Tenth Int'l Conf. on Phenomena in Ionized Gases, Oxford, 394 (1971).

[10] R. M. Measures, J. Quant. Spec. Radiat. Trans. 10, 107 (1970), J. Appl. Phys. 48, 2673 (1977). Also R. M. Measures, et al., Appl. Opt. 18, 1824 (1979).

[11] T. J. McIlrath and T. B. Lucatorto, Phys. Rev. Lett. 38, 1390 (1977).